DOI: https://doi.org/10.33103/uot.ijccce.22.4.5

Medical Image Enhancement Techniques

Dhuha Abd Almoanf[1], Shaimaa H. Shaker[2]
[1,2]Computer Sciences Department, University of Technology, Baghdad, Iraq
[1]cs.19.07@grad.uotechnology.edu.iq, [2]shaimaa.h.shaker@uotechnology.edu.iq

Abstract— *Computed tomography (CT) is used to diagnose diseases and tumors. A special dye called contrast material is used in CT scans to assist emphasize the parts of the body being examined. Therefore, an enhancement technique to improve CT images' degradation is needed. This paper aims to present a method to enhance the quality of Ct-Scan images based on discrete wavelets transform and the Retinex algorithm. The proposed methods are based on the Retinex algorithm parameters or Dark Channel Prior algorithm parameters, according to the output image from preprocessing and discrete wavelets algorithm steps to increase the lightness degree of an image, remove possible noise from the image improve the contrast. The results of experiments of the enhanced image outputted from the Retinex model compared with one outputted from the Dark Channel Prior method. Hence, image quality based on the DCP method is a higher degree of enhanced rate and reasonable rate of noise removal-based enhancement measures, which were SI, MSE, IQI, SNR, and SNR, but was very attentive to the percentage values of IQI and SI. So the DCP with WT was recorded as the highest rate of enhancement.*

Index Terms— *Dark Channel Prior, Image quality assessment, Liver CT, Retinex model, Wavelet Transform.*

I. INTRODUCTION

Computed tomography (CT) is an important diagnostic imaging method for examining a variety of clinical disorders [1]. Various circumstances cause the lowlight effect in the acquired CT scan images, such as faulty scanner settings, which include improper shutter speed (i.e., being too slow or too fast), and incorrect exposure amount, which provides for too high (bright) or too low (dim) exposure. Besides, the environment's illumination is deficient, providing low light, uneven brightness, nighttime, backlight, shadowed background, etc. Because the accepted quality of these images must be improved for better analysis, interpretation, and explanation, lowlight image enhancement methods must be used to reveal the hidden information [2]. The main goal of lowlight enhancement techniques is to restore well-perceived images to a high enough quality that the majority of their essential information is given without causing unexpected artifacts. In 2017, Qinli et al. [3] introduced wavelet decomposition theory that decomposed the original image into four sub-images, including an approximation image (the low-frequency sub-image) and three detail images (the high-frequency sub-images). The low-frequency sub-image (LL) is used in conventional image enhancement methods. Nandhini V. et al.in 2015 [4] presented a method for enhanced contrast based on histogram equalization classification and compared the entropy of that method to the conventional histogram equalization to determine the sum of information contained within the image. Other equalization approaches do not give as much improvement as the proposed method because the clipping and luminance exposure threshold values must be chosen. Shiet al.2017 [5] proposed dark channel prior (DCP), which assumes a highly dark pixel exists in every color channel of the

Received 14/February/2022; Accepted 24/May/2022
 ISSN (Print) 1811-9212 ISSN (Online) 2617-3352

DOI: https://doi.org/10.33103/uot.ijccce.22.4.5

local non-sky patch around all pixels. Li M. et al. in 2018 [6] provided the noise term to the standard Retinex decomposition. The traditional Retinex approach and the reflectance part were utilized to estimate the illumination in this method.

This paper aims to get an enhanced CT image that was degraded with low contrast. So the proposed method depending on discrete wavelet transforms, acts on preprocessing CT scan image followed by Dark Channel Prior or Retinex algorithm. As well as compared the results of the proposed method with other methods to determine the efficiency of this work.

The structure of the paper is divided into the following sections. Section II describes image performance metrics, while section III explains the proposed methodology. Section IV states the work's outcome discusses these results and includes tables to compare the suggested methodology results with other methods in terms of the improvement rate and noise removal. Finally, section V contains the conclusions reached by the research paper and some suggestions for future work.

II. IMAGE PERFORMANCE METRICS

Performance metrics are used to measure the features of an image quantitatively. Mean Square Error (MSE), Peak Signal to Noise Ratio (PSNR), Mean Absolute Error (MAE), Signal to Noise Ratio (SNR), Lightness order error (LOE), Similarity Index (SI), Structural Similarity Index Measure (SSIM), Statistical Pearson Correlation Coefficients and Image Quality Index (IQI) [7][8].

-The Mean Absolute Error is defined as:

$$MAE\frac{1}{n}\sum_{i=0}^{n}|f_i - y_i| \tag{1}$$

It is the difference between original and enhanced images.

-The peak-SNR is defined as:

$$PSNR = 10\ \log_{10}\frac{(L-1)^2}{\frac{1}{N^2}\sum_{r=0}^{N-1}\sum_{c=0}^{N-1}\left[\hat{I}(r,c) - I(r,c)\right]^2} \tag{2}$$

I(r,c) is the original image's pixel brightness., *I ̂(r,c)* The pixel brightness of the manipulated image. N^2 the total number of pixels in the image. *L* is the number of different shades of gray (pixel brightness levels).

-MSE is described as:

$$MSE = \frac{1}{MN}\sum_{r=0}^{M}\sum_{c=0}^{N}\left[\hat{I}(r,c) - I(r,c)\right]^2 \tag{3}$$

N is the pixel's number in the enhanced image. M is the pixel's number in the original image. The average absolute difference in pixel intensity is the Mean Square Error.

-Similarity Index (SI) is described as:

$$SI = \frac{(m_{ab}2xy2m_a m_b)}{(m_a m_b x^2 + y^2 m_a^2 + m_b^2)} \tag{4}$$

m_a is the pixel's number in the enhanced image. mb is the pixel's number in the original image

, while The SSIM is defined as:

$$SSIM(x,y) = \frac{(2\mu_x\mu_y + C)(2\sigma_{xy} + C_2)}{(\mu_x^2 + \mu_y^2 + C_1)(\sigma_x^2 + \sigma_y^2 + C_2)} \tag{5}$$

Received 14/February/2022; Accepted 24/May/2022
 ISSN (Print) 1811-9212 ISSN (Online) 2617-3352

DOI: https://doi.org/10.33103/uot.ijccce.22.4.5

where μ_x The average of *x*,μ_y The average of y, σ_x^2 The variance of x, σ_y^2 The variance of y

σ_{XY} The covariance of x and y, C_1, C_2 To keep a division with a weak denominator stable, use two variables.

-Lightness order error is defined as:

$$LOE = \frac{1}{mn}\sum_{i=1}^{m}\sum_{j=1}^{n} RD(i,j) \tag{6}$$

where RD(i,j) is the pixel's relative order difference.

$$RD(i,j) = \sum_{k=1}^{m}\sum_{l=1}^{n}\Big(U\big(L(i,j),L(k,l)\big) \oplus U\big(L_E(i,j),L_E(k,l)\big)\Big) \tag{7}$$

The maximum of the three color channels is L(k,l), The exclusive-or operator U is a unit step function. [9].

-The image Quality Index (IQI) is defined as:

$$IQI=1-SI \tag{8}$$

The IQI is a metric that compares the pixel discrepancies among two images (img1 & img2), If both the original image (img1-K I j) and the modified image (img2- I I j) are present,) ranging from -1 to 1 are identical, IQI equals 0.

-Pearson Correlation Coefficient (r), also represented as r can determine the degree of association between two sets of rank-ordered pixels of two images.

$$correlation(ij,i1j1)(r) = \frac{\sum_{i=1}^{n}(i1-i)(j1-j)}{\sqrt{\sum_{i=1}^{n}(i1-i)^2}\sqrt{\sum_{i=1}^{n}(j1-j)^2}} \tag{9}$$

Where i1 is the ith pixel's luminance in image1, j1 is the ith pixel's luminance in image2, I is the mean intensity of image1, and j is the mean intensity of image2 [10].

III. PROPOSED METHODS

Enhancement images were applied and considered necessary to improve the quality of images [4], [11]. To enhance CT scan imaging efficiency and obtain an accurate diagnosis. The CT scan image enhancement methodology was done in steps, as shown in *Fig. 1*. All the operations were done using OpenCV Python. The topic can easily be divided into several sub-chapters.

Received 14/February/2022; Accepted 24/May/2022
 ISSN (Print) 1811-9212 ISSN (Online) 2617-3352

DOI: https://doi.org/10.33103/uot.ijccce.22.4.5

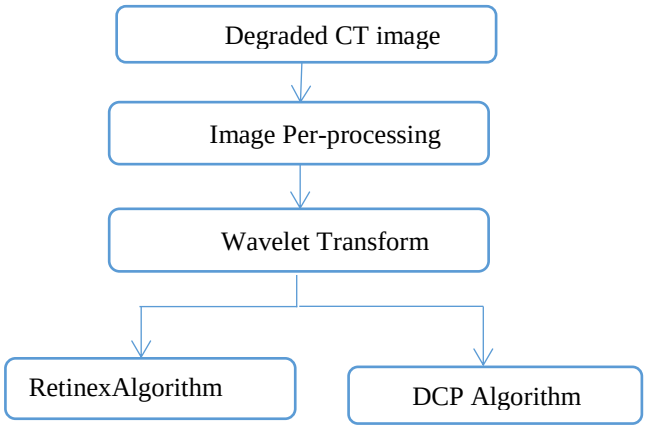

FIG. 1. WORKFLOW OF PROPOSED METHODS.

A. The Proposed Schema

The following section explains the flow of the proposed method with all parameters that need to raise an image's quality. All steps of the proposal are described as some algorithms. The proposed method's main steps are as follows: algorithm1:-

Algorithm 1:Main steps of algorithm
Input: image (512 , 512) Output: enhanced image (E(256,256))

Begin
Read image (i, j)
Call preprocessing-step(image(512,512) //the output is G image//
Call DWTA-step(G) // the output is W image//
Call MSRA-step(W) // the output is E(enhance image//
End

i. Image Capture

The First step is to obtain a CT scan image. A CT scan is a diagnostic imaging technique that creates tomographic (cross-sectional) images (virtual "slices") of a body that used computer-processed mixtures of multiple X-ray metrics taken from different corners, allowing the user to see inside the body without cutting it open. Two datasets are adopted in this study to assess the performance of the proposed method in the experiments and comparisons. The first dataset is collected from the internet website (https://radiologykey.com). The second dataset is a real dataset collected from Baghdad educational hospital /medical city / Radiology department. Then used radiant DICOM viewer, a specialized program for viewing medical images—the size of all images is 512x512 pixels, with the final size of 255x255 pixels.

ii. Image Preprocessing

Image preprocessing is the next step. This step aims to improve and smooth the examination of data in images so that it can be used as input for subsequent steps. Therefore, do selectively remove redundancy from scanned images without disturbing the critical details of the diagnosis process. The image preprocessing includes the following processes algorithm:

The first process is to resize the image to 255×255 pixels. The color image RGB is then converted to a grayscale image in the second step. which saves processing time and allows for faster

Received 14/February/2022; Accepted 24/May/2022

ISSN (Print) 1811-9212 ISSN (Online) 2617-3352

DOI: https://doi.org/10.33103/uot.ijccce.22.4.5

algorithms [12]. The third one is cropping the edges of images to trim the margins that are not captured in the scanner and normalizing the boundaries according to the default scene. The fourth process is the median filter, obtained by relaxing the order statistic for pixel substitution. The statistical properties of noise attenuation, as well as edge and line preservation, are investigated[8]. The trade-off between noise reduction and detail-keeping has been extensively studied.

Definition: Let m = N+1 and *l*, *u* such that $1 \leq l<m<u< 2N+1$. The relaxed median filter with bounds *l* and *u* is described as:

$$Yi = RM_{lu}\{Wi\} = \begin{cases} Xi & if\ Xi \in \left[[Wi]_{(l)}, [Wi]_{(u)}\right] \\ [Wi]_{(m)} & otherwise \end{cases} \quad (10)$$

Where [Wi](m) is the median value of the samples inside the windows Wi.

Xi is the m-dimensional sequence.

Algorithm 2:preprocessing-step
Input: Image (512 , 512)
Output: G(256,256) // noiseless and contrast image //

Begin
Degraded image selected based on the entropy values
I=resize(image,(256,256)) //Resize image 512×512 to image 256×256//
G=COLOR_BGR2GRAY //convert image to a gray level//
Call cropping(G) function //cropping edges of images to trim the margin// Call relaxed median-function(crop(G))//relaxed median filter with bounds*l* &*u* //
End

iii. Wavelet Transform

This step has used the output of preprocessing step as the input to wavelet transforms mapping. A wavelet is a short wave with varying frequency and limited duration. Wavelet can also be defined as a fast-decaying oscillation by building blocks for representing images at varying resolutions.DWT decomposes the input image into sub-band images, including a fictitious low-frequency sub-image (LL) third description images called the high-frequency sub-images (HL, LH, and HH). The Discrete Wavelet Transform (DWT) function is [13-16]:

$$W^s(K, l)=\frac{1}{s}\sum_n \sum_m f(m,n)\psi\left(\frac{m-1}{s}\right)\psi\left(\frac{n-1}{s}\right) \quad (11)$$

Where (k, l) is the position of the wavelet and s is the scale.

iv. Retinex Algorithm

In this step, the Retinex algorithm is used to enhance the approximation images (LL) that get it from the previous step, as follows:

Step1: Images decomposed into reflectance and illumination in the classic Retinex model [17], [18], [19]:

$$I = R \cdot L \quad (12)$$

Where I is the observed image, R and L are the image's reflectance and illumination.

Step2: The logarithmic transformation is utilized by most existing Retinex-based algorithms to reduce computing complexity [19]:

$$log\ I = log\ R + log\ L \quad (13)$$

The log of the image is the sum of the log of reflectance and the log of illumination.

Step3: The reflectance is calculated as follows:

$$\log \mathrm{R} = \log \mathrm{I} - \log \mathrm{L} \quad (14)$$

Step4: Estimate the reflectance by:

$$\mathrm{R} = \exp(\log \mathrm{I} - \log \mathrm{L}) \quad (15)$$

Received 14/February/2022; Accepted 24/May/2022

 ISSN (Print) 1811-9212 ISSN (Online) 2617-3352

DOI: https://doi.org/10.33103/uot.ijccce.22.4.5

v. Dark Channel Prior Algorithm (DCP)

This prior algorithm is used for the imaging model hazing, So estimate the haze thickness and recuperate a premium haze-free image. A mixture of hazy images, as a result, is the power of the prior. DCP is derived from the characteristic of images that have at least one color and an illumination value within a certain point is on the brink of zero. Based on the DCP, the dehazing is accomplished through four significant steps:

(i) Atmospheric light estimation
(ii) Transmission map estimation
(iii) Transmission map refinement
(iv) Image reconstruction

The dark-field imaging system for CT dimension is depending upon a tandem system of "Bragg- and Laue-case crystals and 2-D determiners, with rocking-curve-fitting and multi termes functions, used to extract refraction data from the measured criss-cross concentration. Soft tissue reconstructed images are shown and described. [21], [22].

IV. RESULTS AND DISCUSSION

This section presents the results of the proposed method and its comparison with three different techniques. The images obtained from Baghdad educational hospital are in DICOM format with size 512. Radiant DICOM Viewer is used to converting the DICOM images to jpeg format to process the images in python. The results of the processes are enhanced images with a size of 256. The suggested method's effectiveness was assessed by comparing the enhancement results to those obtained using specific lowlight picture enhancement methods. The results of these comparisons are evaluated through custom metrics, that is, peak signal-to-noise ratio (PSNR) metrics[23], structural similarity index measure (SSIM)[24],[25],[26], Mean Square Error(MSE)[27],[28], Similarity Index (SI), Image Quality Index (IQI)and Lightness order error (LOE)[29],[30]. Tables I-IV display the metrics scores for the comparatives. *Fig. 2* presents the original image with low quality that's clear as in Table VI such that the entropy of the original image is lower than other images in *Fig. 2*. So the original image has a lower mean than other images in *Fig. 1* as shown in Table II. Table I shows the results of the PSNR measure, where a higher value indicates a better enhancement. Table I, Table II, Table III, Table IV, Table V, and Table VI, according to *Fig. 2*, *Fig. 3*, and *Fig. 4*, show some comparisons of the results of the proposed method with other methods. According to Table I, II, III, V, DCP is the best enhancement method because the average of the PNSR measure is higher than others, and the average of the MSE measure is lower than others. The average of SSIM measures is higher than others. That means that the original image is highly similar with results enhancing the image and the average IQI measure is lower than others. This means the enhanced image is too close to the original image. So from these tables, the measurement results of the proposed method using wavelets transform followed by DCP are near the best results.

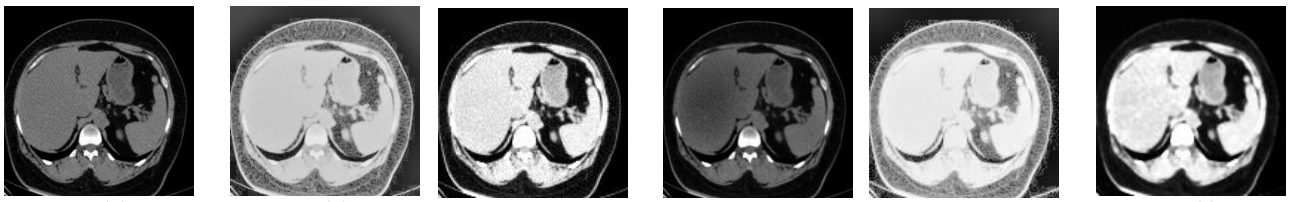

(A) (B) (C) (D) (E) (F)

FIG. 2. THE COMPARISON OUTCOMES (A) ORIGINAL IMAGE; THE FOLLOWING IMAGES ARE ENHANCED BY: (B) RETINEX, (C) WAVELET TRANSFORM,(D) DCP, (E) WT AND RETINEX(F) WT AND DCP.

Received 14/February/2022; Accepted 24/May/2022
 ISSN (Print) 1811-9212 ISSN (Online) 2617-3352

DOI: https://doi.org/10.33103/uot.ijccce.22.4.5

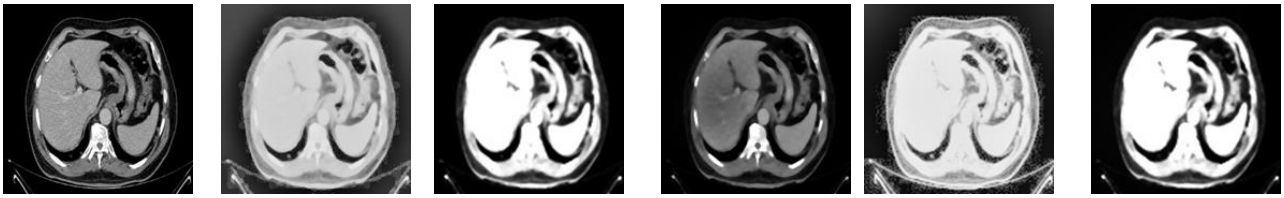

(A) (B) (C) (D) (E) (F)

FIG. 3. THE COMPARISON OUTCOMES (A) ORIGINAL IMAGE; THE FOLLOWING IMAGES ARE ENHANCED BY: (B) RETINEX, (C) WAVELET TRANSFORM,(D) DCP, (E) WT AND RETINEX(F) WT AND DCP.

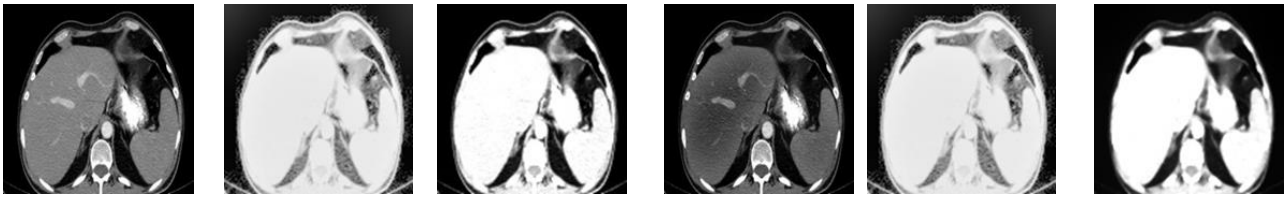

(A) (B) (C) (D) (E) (F)

FIG. 4. THE COMPARISON OUTCOMES (A) ORIGINAL IMAGE; THE FOLLOWING IMAGES ARE ENHANCED BY: (B) RETINEX, (C) WAVELET TRANSFORM,(D) DCP, (E) WT AND RETINEX(F) WT AND DCP.

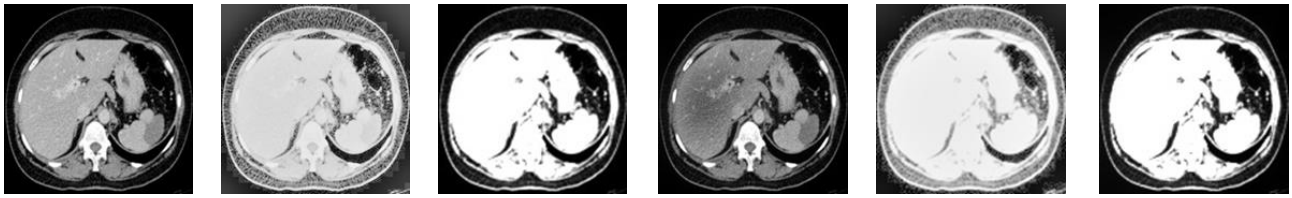

(A) (B) (C) (D) (E) (F)

FIG. 5. THE COMPARISON OUTCOMES (A) ORIGINAL IMAGE; THE FOLLOWING IMAGES ARE ENHANCED BY: (B) RETINEX, (C) WAVELET TRANSFORM,(D) DCP, (E) WT AND RETINEX(F) WT AND DCP.

TABLE I. THE PSNR SCORES OF RESULTS OF EXPERIMENTAL IMAGES

Methods	Figure2	Figure3	Figure4	Figure5	Average
Retimex	27.6299	27.7402	27,7170	27.7084	27.6631
Wavelet	29.1403	29.9092	30.3506	28.7496	29.6708
DCP	31.0821	30.8619	30.2661	30.7571	31.3222
WT+Retnix	28.6071	27.9536	27.9718	28.0805	28.1532
WT+DCP	29.8083	30.6861	30.1374	28.4406	29.7681

TABLE II. THE MSE SCORES OF RESULTS OF EXPERIMENTAL IMAGES

Methods	Figure2	Figure3	Figure4	Figure5	Average
Retinex	122.2250	109.4097	109.9765	110.2140	118.8717
Wavelet	79.2577	66.3983	59.9813	86.7184	71.1701
DCP	50.6828	53.3191	61.1596	54.6085	49.4229
WT+Retnix	89.6110	104.1626	103.727	101.1647	99.6664
WT+DCP	67.9592	55.5220	62.9987	93.1146	69.8986

TABLE III. THE SSIM SCORES OF RESULTS OF EXPERIMENTAL IMAGES

Methods	Figure2	Figure3	Figure4	Figure5	Average
Retinex	0.3733	0.2830	0.4269	0.4305	0.3886
Wavelet	0.6992	0.6707	0.6817	0.6617	0.6942
DCP	0.9699	0.7559	0.9424	0.9469	0.962
WT+Retnix	0.2828	0.2409	0.3167	0.3177	0.2895
WT+DCP	0.6193	0.6379	0.5344	0.6041	0.5989

Received 14/February/2022; Accepted 24/May/2022

ISSN (Print) 1811-9212 *ISSN (Online) 2617-3352*

DOI: https://doi.org/10.33103/uot.ijccce.22.4.5

TABLE IV. THE LOE SCORES OF RESULTS OF EXPERIMENTAL IMAGES

Methods	Figure2	Figure3	Figure4	Figure5	Average
Retinex	208.3868	269.7500	243.5988	202.1460	230.9704
Wavelet	43.5936	52.7204	121.3104	152.3092	92.4834
DCP	130.1504	55.4172	211.3148	135.3092	133.079
WT+Retnix	178.9340	233.7800	296.5568	292.9348	250.5514
WT+DCP	122.0956	175.6628	249.8480	178.8884	181.6237

TABLE V. THE IQI SCORES OF RESULTS OF EXPERIMENTAL IMAGES

Methods	Figure2	Figure3	Figure4	Figure5	Average
Retinex	0.6267	0.7169	0.5731	0.5695	0.6115
Wavelet	0.3008	0.3292	0.3183	0.3383	0.3058
DCP	0.0301	0.2440	0.0576	0.0531	0.038
WT+Retnix	0.7171	0.7591	0.6832	0.6823	0.7104
WT+DCP	0.3806	0.3620	0.4655	0.3958	0.4009

TABLE VI. ENTROPY RESULT FOR THE PROPOSED METHODS

	Original image	Wavelet image	Enhanced image(WT+DCP)	Enhanced image(WT+Retinx)
Fig2	6.03	6.60	7.20	6.85
Fig3	5.72	5.21	6.37	6.09
Fig4	6.04	5.21	6.75	5.59
Fig5	6.64	5.35	6.75	5.58

TABLE VII. MEAN RESULT FOR THE PROPOSED METHODS

	Original image	Wavelet image	Enhanced image(WT+DCP)	Enhanced image(WT+Retinx)
Fig2	54.88	104.32	162.06	103.29
Fig3	60.81	102.83	130.50	83.60
Fig4	72.71	130.96	159.61	129.96
Fig5	84.34	132.53	173.40	132.03

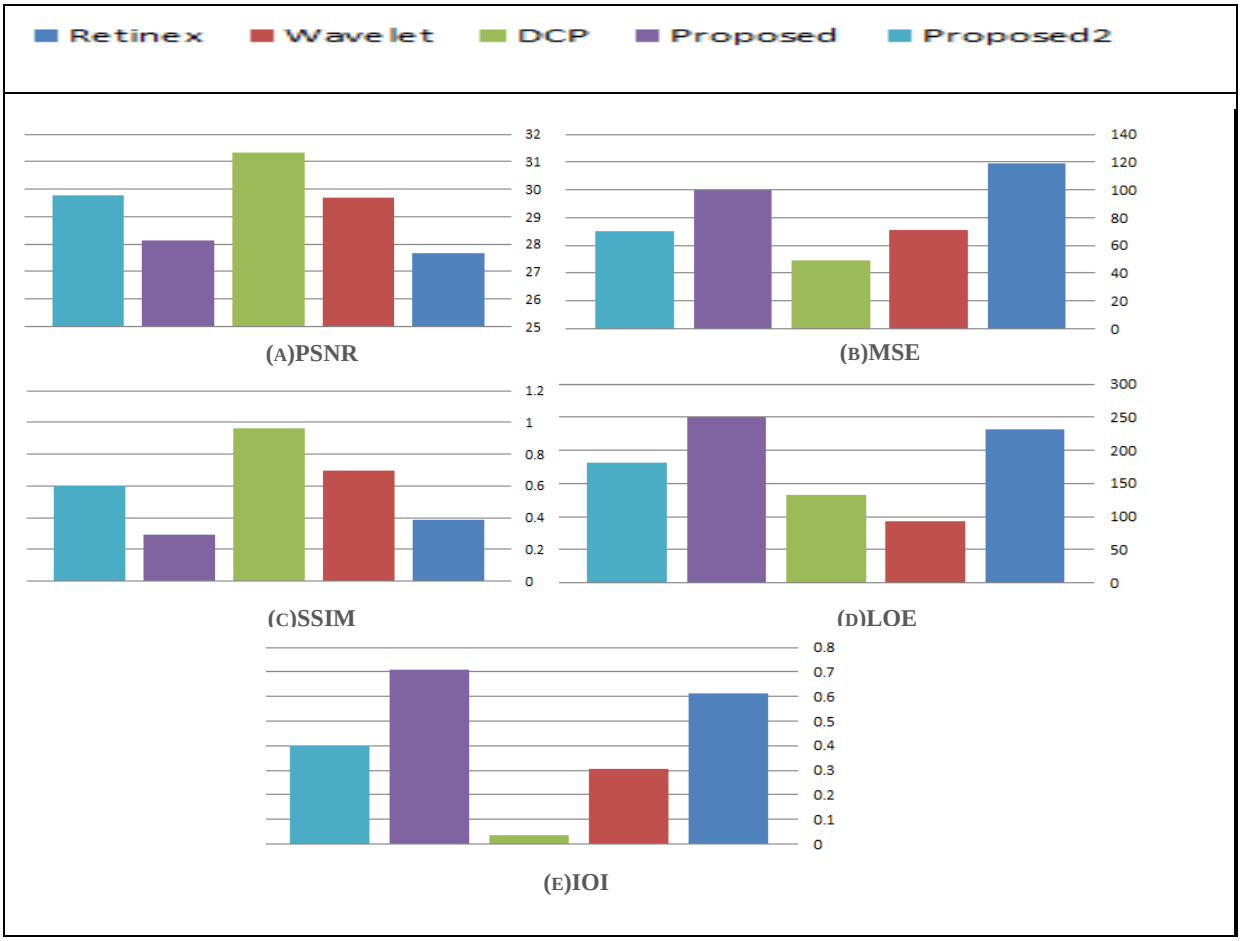

FIG. 6. AVERAGE PSNR, MSE, SSIM, LOE, AND IOI RESULTS FOR DIFFERENT METHODS.

Received 14/February/2022; Accepted 24/May/2022

ISSN (Print) 1811-9212 *ISSN (Online) 2617-3352*

DOI: https://doi.org/10.33103/uot.ijccce.22.4.5

The entropy of the original image (in *Fig.1* and *Fig. 2*) is less than the entropy of the enhanced image produced from the preprocessing image that transforms by wavelets, the preprocessing image that changes by wavelets followed by DCP algorithms, and preprocessing image that transformed by wavelets followed by Retinex algorithm, as shown in Table VI. Entropy is a statistic used to determine visual content, with a higher value suggesting a more detailed image. In contrast, the entropy of the original image(in *Fig. 3* and *Fig. 4*) is greater than the entropy of the enhanced image produced from the preprocessing image that transforms by wavelets, algorithms, and preprocessing image that changes by wavelets followed by Retinex algorithm but less than the entropy of enhanced image produced from the preprocessing image that transforms by wavelets followed by DCP. So entropy is a measure of the quantity of random information in the image. The average intensity, density, or gray level of an image is represented by its mean. The image created by mean removal describes the edges and gray level fluctuations around the mean. A decrease in the mean value causes an increase in image enhancement. So these results are shown in Table VII. Figures 2-5 show the outcomes of applying the proposed method and other methods to different degraded images. *Fig. 6* represents Tables I-IV providing graphs showing average scores. The experiments revealed that the proposed method produced excellent and medium-enhanced CT images. When the Similarity Index is more than 40% when evaluated in percentages, it is advised that an improved image is regarded as comparable to the original image. Hence, the proposed method's SSIM is around 28% and 60% for an average of all images in Table IV.

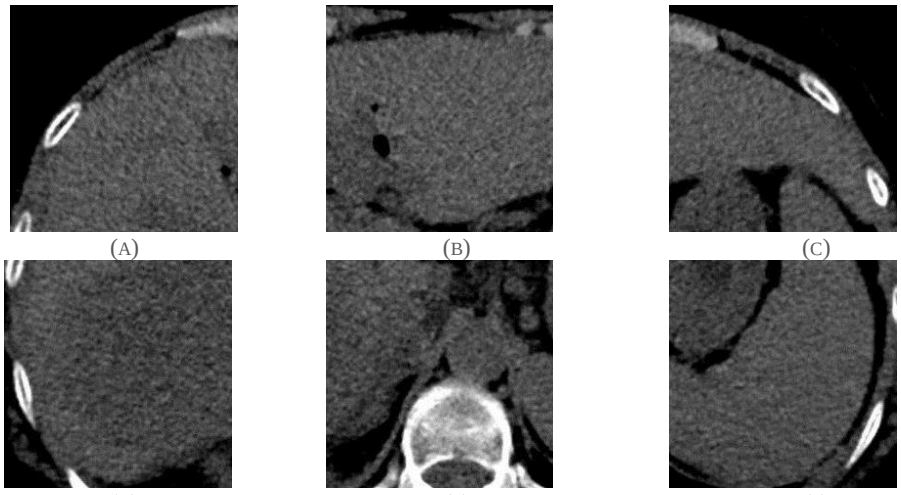

FIG. 7. CT-SCAN IMAGE SPLIT FOR SIX-PART (A) PART1, (B) PART2, (C) PART3, (D) PART4, (E) PART5, (F) PART6.

Received 14/February/2022; Accepted 24/May/2022
 ISSN (Print) 1811-9212 *ISSN (Online) 2617-3352*

DOI: https://doi.org/10.33103/uot.ijccce.22.4.5

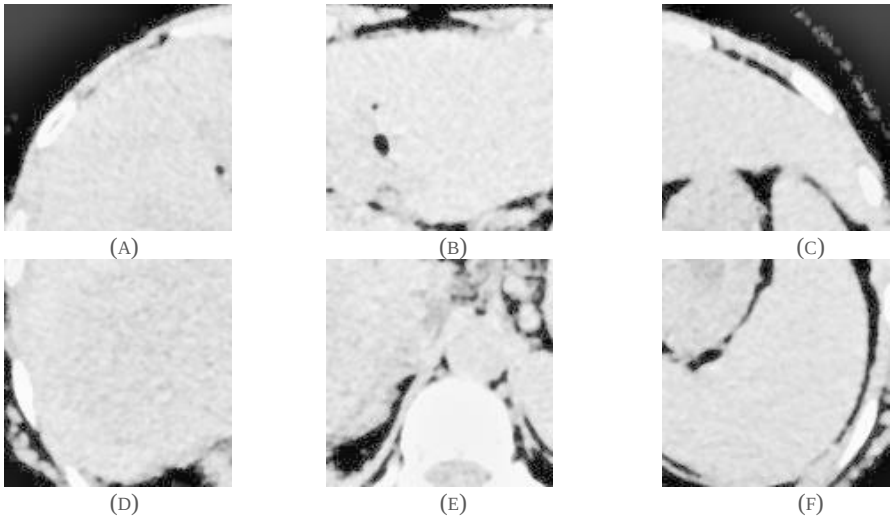

(A) (B) (C)

(D) (E) (F)

FIG. 8.CT-SCAN IMAGE PROCESSED BY DW AND RETINEX METHOD.

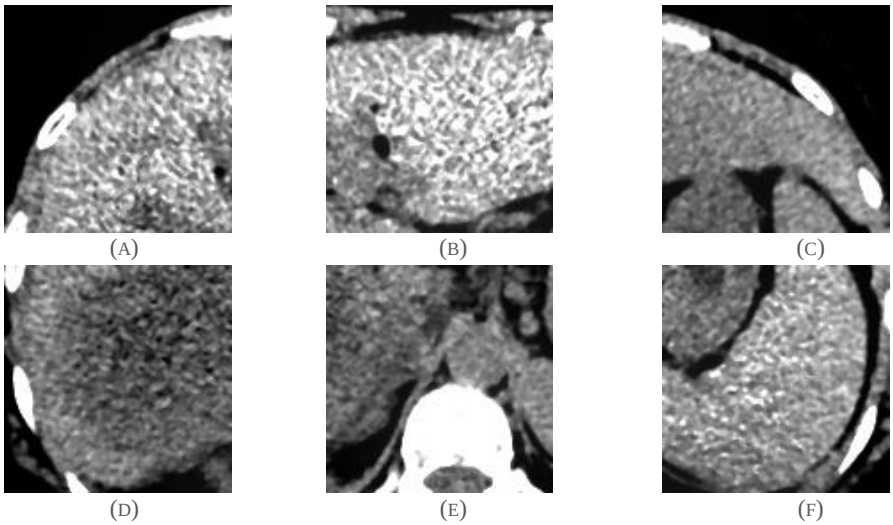

(A) (B) (C)

(D) (E) (F)

FIG. 9. CT-SCAN IMAGE PROCESSED BY DW AND DCP METHOD.

TABLE VIII. RESULT OF THE PROPOSED METHODS FOR PART1

methods	PSNR	MSE	SSIM	LOE	IOI	Entropy	Mean
WT+Retnix	27.95	104.07	0.3317	230.64	0.6682	6.24	174.56
WT+DCP	29.07	80.44	0.6754	128.99	0.3245	6.70	113.64

TABLE IX. RESULT OF THE PROPOSED METHODS FOR PART2

methods	PSNR	MSE	SSIM	LOE	IOI	Entropy	Mean
WT+Retnix	27.67	111.16	0.5351	205.24	0.5812	5.57	215.70
WT+DCP	27.76	108.90	0.4187	131.11	0.4648	7.62	153.60

TABLE X. RESULT OF THE PROPOSED METHODS FOR PART3

methods	PSNR	MSE	SSIM	LOE	IOI	Entropy	Mean
WT+Retnix	27.92	104.93	0.3112	207.87	0.6887	6.73	165.54
WT+DCP	28.96	82.46	0.7829	179.66	0.2170	6.55	88.30

TABLE XI. RESULT OF THE PROPOSED METHODS FOR PART4

methods	PSNR	MSE	SSIM	LOE	IOI	Entropy	Mean
WT+Retnix	27.61	112.70	0.3848	180.26	0.6151	5.68	209.32
WT+DCP	28.22	97.92	0.7773	241.12	0.2226	7.13	89.98

Received 14/February/2022; Accepted 24/May/2022

 ISSN (Print) 1811-9212 *ISSN (Online) 2617-3352*

DOI: https://doi.org/10.33103/uot.ijccce.22.4.5

TABLE XII. RESULT OF THE PROPOSED METHODS FOR PART5

methods	PSNR	MSE	SSIM	LOE	IOI	Entropy	Mean
WT+Retnix	27.73	109.42	0.3549	153.76	0.6450	6.46	206.86
WT+DCP	29.07	80.44	0.6781	190.31	0.3218	6.93	117.49

TABLE XIII. RESULT OF THE PROPOSED METHODS FOR PART6

methods	PSNR	MSE	SSIM	LOE	IOI	Entropy	Mean
WT+Retnix	27.66	111.24	0.4020	168.30	0.5979	5.80	205.05
WT+DCP	27.79	107.93	0.6385	107.68	0.3614	7.60	123.79

Fig. 7 shows the liver CT scan image split into six-part and each part is enhanced by the two proposed methods, the results of enhancing shown in *Fig. 8* and *Fig.9.* After the enhancement, each part's experimental results are shown in Tables VIII-XIII.

V. CONCLUSIONS

There are many different image quality metrics implemented for getting the quality of an image. The resulting image is improved since the different samples of images evaluated are based on various measures, so the proposed method's result is close to the others compared to other methods. The images with and without image enhancement schemes considerably differ in the results. This is evident from the experimental result presented. The visual details are visible to the naked eye with the image enhancement algorithm applied.

REFERENCES

[1] D.T. Ginat and R. Gupta, "Advances in computed tomography imaging technology," Annual review of biomedical engineering, vol. 16, pp. 431-453, July 2014.

[2] R. Liaqat, A. I. Majeed, M. N. Malik, A. Shafi, S. Z. Shah, B. Liaqat, "Confronting our mistakes: A comprehensive evaluation of radiographic errors in digital chest radiography among adult population in a public sector hospital," Annals of PIMS-Shaheed Zulfiqar Ali Bhutto Medical University, vol. 17, pp. 129-133, June 2021.

[3] Z. Qinli, S. Shutingb, S. Xiaoyunc, and G. Qi, "A Novel Method of Medical Image Enhancement Based on Wavelet Decomposition," Automatic Control and Computer Sciences, vol. 15, pp. 263–269, May 2017.

[4] V. Nandhini, R. Pratheepa, N. Anjana and V. Elamaran, "A Novel Approach for Contrast Enhancement using Image Classification and Subdivision based Histogram Equalization,", Indian Journal of Science and Technology, vol. 8, PP.1-6 ,Nov. 2015.

[5] L. Shi, L. Ynag, S. Chu, X. Cui, J. Yang, Y. Yang, B. Zhao and M. Fu, "Image haze removal using dark channel prior and minimizing energy function," in 2017 IEEE 2nd Information Technology, Networking, Electronic and Automation Control Conference (ITNEC). IEEE, pp. 256-259, Dec. 2017.

[6] M. Li, J. Liu, W. Yang, X. Sun and Z. Guo, "Structure-revealing lowlight image enhancement via robust retinex model," IEEE Transactions on Image Processing, vol. 27, pp. 2828-2841, June 2018.

[7] U.Y. Al-Najjar, D. C. Soong, "Comparison of Image Quality Assessment: PSNR, HVS, SSIM, UIQI," International Journal of Scientific & Engineering Research, Vol. 3, pp. 1-5, August 2012.

[8] Z. Afrose, "Relaxed Median Filter: A Better Noise Removal Filter for Compound Images", International Journal on Computer Science and Engineering (IJCSE), vol. 4, pp. 1376-1382, July 2012.

[9] S. Wang, J. Zheng, H. Hu and B. Li, "Naturalness Preserved Enhancement Algorithm for Non-Uniform Illumination Images", IEEE Transactions on Image Processing, vol. 22, pp. 3538 – 3548, September 2013.

[10] M. Pedersen, J.Hardeberg, "Full-Reference Image Quality Metrics: Classification and Evaluation", Computer Graphics and Vision, vol. 7, pp. 1–80, January 2012.

[11] H. A. R. Akkar and S. Q. Hadad, "Diagnosis of Lung Cancer Disease Based on Back-Propagation Artificial Neural Network Algorithm", Engineering and Technology Journal, vol. 38, pp. 184-196, December 2020.

[12] Z. F. Jabr and M.A.A. Hasan, "Diagnosing of some hepatic lesions from light microscope images based on morphological and texture features", Indonesian Journal of Electrical Engineering and Computer Science(IJEECS), vol. 18, pp. 995-1003, May 2020.

[13] D. Zhang, "Wavelet transform", In Fundamentals of Image Data Mining. Springer, Cham, 2019, pp. 35-44.

Received 14/February/2022; Accepted 24/May/2022

 ISSN (Print) 1811-9212 *ISSN (Online) 2617-3352*

DOI: https://doi.org/10.33103/uot.ijccce.22.4.5

[14] M. E. Khani, D. P. Winebrenner, and M. H. Arbab, "Phase function effects on identification of terahertz spectral signatures using the discrete wavelet transform," IEEE Transactions on Terahertz Science and Technology, vol. 10, pp. 656-666,May, 2020.

[15] A. Al-Obaidi, S. H. Alnajjar, M. Nsai, H. Sharabaty, "Classification of Multi Heart Diseases With Android Based Monitoring System," Iraqi Journal of Computers, Communications, Control and Systems Engineering (IJCCCE), vol. 20, pp. 14-22, April 2020.

[16] I. A. Abdul-Jabbar, "Face Image Enhancement using Wavelet Denoising and Gabor Filters," Iraqi Journal of Computers, Communications, Control and Systems Engineering (IJCCCE), vol. 16, pp. 104-117, March 2016.

[17] A. S. Parihar and K. Singh. "A study on Retinex based method for image enhancement," in 2018 2nd International Conference on Inventive Systems and Control (ICISC). IEEE, pp. 619-624, January 2018.

[18] Y. Gao, H. Hu, B. Li and Q. Guo, "Naturalness preserved nonuniform illumination estimation for image enhancement based on retinex," IEEE Transactions on Multimedia, vol. 20, no. 2, pp. 335-344, Aug. 2017.

[19] M. Li, J. Liu, W. Yang, X. Sun and Z. Guo, " Structure-Revealing Low-Light Image Enhancement via Robust Retinex Model," IEEE Transactions on Image Processing, vol.27, pp. 2828-2841, February 2018.

[20] J. Xu, Y. Hou, D. Ren, L. Liu, F. Zhu, M. Yu ,H. Wang and Ling Shao, "Star: A structure and texture aware retinex model," IEEE Transactions on Image Processing, vol.29, pp. 5022-5037, March, 2020.

[21] N. Sunaguchi1, T. Yuasa, Q. Huo, S. Ichihara and M. Ando, "X-ray refraction-contrast computed tomography images using dark-field imaging optics", Applied Physics Letters, vol. 97, pp. 153701, October 2010.

[22] Y. Peng, K. Cao and P. C. Cosman. "Generalization of the dark channel prior for single image restoration," IEEE Transactions on Image Processing, vol. 27, pp. 2856-2868, June 2018.

[23] K. Joshi, R. Yadav and S. Allwadhi. "PSNR and MSE based investigation of LSB." 2016 International Conference on Computational Techniques in Information and Communication Technologies (ICCTICT). IEEE, 2016, pp. 280-285.

[24] A. A.Kareem, A. S. Rahma and H. H. salih, "A Statistical Image Noise Removal Adaptive Filter Using Rejection Test with F-Distribution," Engineering and Technology Journal, vol. 32, pp. 302-312, January 2014.

[25] D. Brunet, E. R. Vrscay and Z. Wang. "On the mathematical properties of the structural similarity index," IEEE Transactions on Image Processing, vol. 21, pp. 1488-1499, October 2011.

[26] L. G. More, M. A. Brizuela, H. L. Ayala, D. P. Pinto-Roa and J. L. V. Noguera. "Parameter tuning of CLAHE based on multi-objective optimization to achieve different contrast levels in medical images," 2015 IEEE International Conference on Image Processing (ICIP). IEEE, Sept. 2015, pp. 4644-4648.

[27] U. Sara, M. Akter and M. S. Uddin. "Image quality assessment through FSIM, SSIM, MSE and PSNR—a comparative study," Journal of Computer and Communications, vol. 7, pp. 8-18, March 2019.

[28] Z. A. A. Alyasseri, A. T. Khader, M. A. Al-Betar, A. K. Abasi and S. N. Makhadmeh. "EEG signals denoising using optimal wavelet transform hybridized with efficient metaheuristic methods," IEEE Access, pp. 10584-10605, December 2019.

[29] Y. Zhang, H. Liu, N. Huang and Z. Wang. "Dynamical stochastic resonance for non-uniform illumination image enhancement," IET Image Processing, vol. 12, pp. 2147-2152, December 2018.

[30] X.Guo, Y. Li and H. Ling. "LIME: Lowlight image enhancement via illumination map estimation," IEEE Transactions on image processing, vol. 26, pp. 982-993, December 2016.

Received 14/February/2022; Accepted 24/May/2022

 ISSN (Print) 1811-9212 *ISSN (Online) 2617-3352*